MAPPING THERMAL FLUX BOUNDARIES SURROUNDING PERMANENTLY SHADOWED REGIONS (PSRS) AT THE LUNAR SOUTH POLE. C. J. Ahrens[1] and N. E. Petro[1], [1]NASA Goddard Space Flight Center, Solar System Exploration Division, Greenbelt, MD (Caitlin.ahrens@nasa.gov).

Introduction: It is important to not only detect water ice remotely at the lunar poles, but it is also critical to constrain the thermal environment that controls what volatiles are present in-situ. PSRs are relatively colder than the average lunar surface, reaching maximum temperatures < 100 K [1]. With such extremely low temperatures, these PSRs have the potential to trap and accumulate water ice and other frozen volatiles [2-3] and retain them for hundreds to millions of years [4]. The surface temperatures at these PSRs are largely controlled by reflected sunlight and irradiated infrared light from adjacent topography [5-6]. However, the localized thermal environment in relation to these lunar PSRs (Permanently Shadowed Regions; and the proximal boundary borders of the PSR) have yet to be examined.

For this study, PSR thermal boundaries are defined as an area of some proximal distance from the mapped PSR boundary that shows some extreme temperature variations comparable to the PSR. These boundaries give us an opportunity to observe the PSR thermal environment and the thermal instability of the environment in which the PSR is situated. That is, temperature variation could be more extreme on one portion of the PSR than the rest of the area. These boundaries can also give us insight into how PSR volatile insolation works or how the thermal environment influences the accumulation/sublimation of the interior PSR. These temperature changes can vary on Diviner instrumentation scales, though we need higher resolution, more localized data on a smaller temporal and spatial scale, in which VIPER (Volatiles Investigating Polar Exploration Rover) can provide [7].

The objective of this study is to understand the immediate thermal boundary surrounding the PSRs and the thermal flux differences between the PSR and boundary, and if there is a difference in thermal flux boundaries at different geographical locations at the lunar south pole.

Methods: The lunar south pole mapping will use LROC WAC (100 m/pixel) and NAC (> 0.5 m/pixel) images combined with bolometric temperature maps from Diviner (240 m/pixel), which are archived on the PDS and available at LROC QuickMap.

Once the Diviner bolometric temperatures are recorded at a PSR and a ~2 km boundary around the PSR, the difference in maximum summer and maximum winter temperatures (ΔT) are used to determine the heat transfer Q (in units of W):

$$Q = \frac{kA(\Delta T)}{d}$$

Where k is the thermal conductivity (0.000461 – 0.0093 W m-1 K-1) from [8], A is the area of the PSR and the boundary, and d is a uniform thickness (in this study, we used 0.02 m for the PSR). Q is then used to determine the surface thermal flux as:

$$Q_{IR} = \frac{Q}{A}$$

Determining the thermal surface flux of a PSR and its surroundings provides insight into the stability of the regolith heat retention, especially for the preservation or destruction of PSR water ice and other volatiles over short timescales.

Preliminary Results: These temperature variations can possibly influence volatile behavior within and around the PSR. For the sake of example, the maximum summer temperature and maximum winter temperature are shown in Figure 1A and 1B, respectively. In the center of this PSR, the temperatures range from 55 – 104 K, which can potentially have H_2O, CO_2, and SO_2 ices [9]. To the southeastern boundary, this temperature range increases up to 240 K, which can have a wider spread of possible volatiles, such as methanol, sodium, and sulfur.
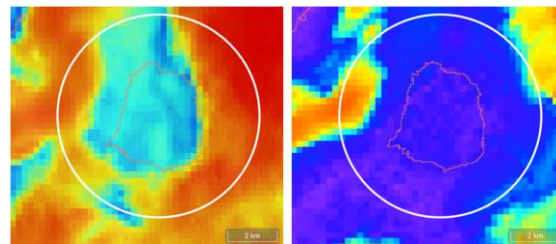

Figure 1: Example of small PSR to the west of Nobile crater (PSR1 in this report). Left: Maximum summer temps from Diviner; Right: Max winter temps from Diviner. White circle: boundary for preliminary work for thermal flux differences at the PSR boundary. Scale bar at 2 km.

In using the equations stated, we preliminarily measured the thermal flux of three PSRs in the lunar south pole. From Table 1, we observed lower thermal fluxes within the PSRs, as expected, with slightly more thermal flux happening in either the north or south portion of the thermal boundaries. The average Q_{IR} differences between the PSR and the thermal boundary was 1.4 for PSR1, 0.5 for PSR2, and 0.2 for PSR3. Further work will look at more PSRs with thermal and spatial differences in these thermal boundaries across different PSR locations.

Table 1: Example PSRs and thermal boundary locations ~2 km from the PSR with measured Diviner temperatures (maximum summer and maximum winter) to determine the thermal flux.

Designation	Lat	Lon	Max Summer [K]	Max Winter [K]	Thermal flux [W m-2]
PSR1	-86.92	48.22	108.7	53.6	1.270055
PSR1 North			118.3	70.6	2.656347305
PSR1 South			208	56.6	3.274465116
PSR1 East			251	60.7	2.2122375
PSR1 West			218	88.9	2.554531915
PSR2	-89.5	282.56	130	113	0.39185
PSR2 North			228.7	152.4	0.94612
PSR2 South			279.5	207	0.812349398
PSR2 East			204.7	169	0.897324324
PSR2 West			241.4	162.3	0.855383721
PSR3	-83.08	350.54	138	125	0.29965
PSR3 North			254	216	0.44175
PSR3 South			300.7	268	0.543053571
PSR3 East			200	104	0.5952
PSR3 West			278	228.7	0.463121212

Summary: We find that temperature variations associated with the accumulation of volatiles within and proximal to lunar PSRs can be verified with surface thermal flux calculations. The thermal flux measurements further our understanding of thermal stability and cold trapping. These PSRs and their thermal boundaries have the potential to answer key questions as to the formation of these PSRs, volatile distribution and regolith properties.

This investigation is also relevant to the upcoming VIPER mission as it traverses along a PSR locality near Nobile crater. The in-situ thermal regolith data provided by the TRIDENT drill integrated with Diviner thermal data should help address the questions surrounding the thermal environments and boundaries at these PSRs.

References: [1] Gladstone, G.R., et al. (2010) Space Sci. Rev.150(1-4), 161–181. [2] Lawrence, D. J. (2017). JGR: Planets, 122(1), 21-52. [3] Li, S., et al., (2018) PNAS, 115 (36), 8907-8912. [4] Siegler, M. A., Keane, J. T., & Paige, D. A. (2018). Lunar Polar Volatiles, 2087, 5038. [5] Ingersoll, A., et al. (1992) Icarus, 100, 40-47. [6] Vasavada, A., et al. (1999) Icarus, 141, 179-193. [7] Colaprete, A., et al. (2019, December). AGU Fall Meeting Abstracts (Vol. 2019, pp. P34B-03). [8] Siegler, M., et al. (2015) Icarus, 255, 78-87. [9] Landis, M. E., et al. (2022) PSJ, 3(2), 39.